PROTEINS
STRUCTURE ■ FUNCTION ■ BIOINFORMATICS

Cold unfolding of β-hairpins: a molecular-level rationalization

Angelo Riccio,[1] and Giuseppe Graziano[2]*

[1] Dipartimento di Scienze Applicate, Università di Napoli "Parthenope", Centro Direzionale Isola C4, 80143 Napoli, Italy
[2] Dipartimento di Scienze Biologiche ed Ambientali, Università del Sannio, Via Port'Arsa 11 - 82100 Benevento, Italy

ABSTRACT

Isolated *β*-hairpins in water have a temperature dependence of their conformational stability qualitatively resembling that of globular proteins, showing both cold and hot unfolding transitions. It is shown that a molecular-level rationalization of this cold unfolding can be provided extending the approach devised for globular proteins (Graziano G. Phys Chem Chem Phys 2010; 12:14245-14252). The decrease in the solvent-excluded volume upon folding, measured by the decrease in the solvent accessible surface area, produces a gain in configurational/translational entropy of water molecules that is the main stabilizing contribution of the folded conformation. This always stabilizing Gibbs energy contribution has a parabolic-like temperature dependence in water and is exactly counterbalanced at two temperatures (i.e., the cold and hot unfolding temperatures) by the always destabilizing Gibbs energy contribution due to the loss in conformational degrees of freedom of the peptide chain.

Proteins 2011; 00:000–000.

Key words: β-hairpin; cold unfolding; solvent-excluded volume; solvent accessible surface area.

INTRODUCTION

It is well established that globular proteins show two unfolding transitions: a cold denaturation and a hot denaturation.[1–5] Cold denaturation is an intriguing phenomenon because a globular protein unfolds on lowering the temperature with heat release and entropy decrease.[1–5] It is widely recognized that cold denaturation is a consequence of the fundamental role played by the hydrophobic effect for the conformational stability of globular proteins.[6,7] However, this has not really produced a molecular-level rationalization because the physical mechanism of the hydrophobic effect is still a debated argument (for more see the Appendix).[8,9]

Recently, one of us has provided a rationalization of cold denaturation[10] by recognizing that two fundamental factors determine the thermodynamic stability of globular proteins in aqueous solution: (a) the large decrease in the solvent-excluded volume upon folding that produces a large increase in the configurational/translational entropy of water molecules, stabilizing the folded conformation; (b) the large decrease in the conformational degrees of freedom of the polypeptide chain upon folding, destabilizing the folded conformation. The increase in the configurational/translational entropy of water molecules upon folding depends on temperature and decreases on lowering the temperature, in particular below the temperature of maximum density, TMD = 3.98°C, of water. So cold denaturation occurs at the temperature where the stabilizing gain in configurational/translational entropy of water molecules is balanced by the destabilizing loss in conformational entropy of the polypeptide chain.[10]

In recent years it has been shown that also monomeric peptide helices and isolated β-hairpins undergo both cold and hot unfolding transitions.[11–15] In particular, β-hairpins constitute an important class of protein structural elements, and it was found that an unconstrained 16-residue (i.e., KKYTVSINGKKITVSI) peptide folds in water to form a β-hairpin (i.e., residues 1–6 form the first strand, residues 7–10 form the β-turn, and residues 11-16 form the second strand), mimicking the two-stranded anti-parallel β-sheet DNA binding motif of the *met* repressor dimer.[12] Circular dichroism and NMR measurements indicate that this β-hairpin has the maximal stability at 303 K and unfolds at both low and high temperatures.[12] The conformational transitions are well described by the reversible two-state model, and the cooperativity should be due to inter-strand interactions, such as H-bonds and van der Waals contacts between nonpolar side chains at positions 3, 5, 12, and 14. It is worth noting that point mutations, introduced in the original sequence of the 16-residue β-hairpin (for instance, Y3L and I16A), do not modify these general features.[12–15] The burial of hydrophobic surface in the fully folded

*Correspondence to: Giuseppe Graziano, Dipartimento di Scienze Biologiche ed Ambientali, Università del Sannio, Via Port'Arsa 11 – 82100 Benevento, Italy. E-mail: graziano@unisannio.it.
Received 12 October 2010; Revised 3 December 2010; Accepted 14 January 2011
Published online 21 January 2011 in Wiley Online Library (wileyonlinelibrary.com). DOI: 10.1002/prot.22997

β-hairpin state is not large, emphasizing a failure of the classical explanation of cold denaturation: the latter occurs when the unfolded state has a heat capacity larger than that of the folded state as a consequence of the exposure to water contact of a large amount of nonpolar side chains.[1–3] Actually, the large positive change in heat capacity upon unfolding cannot be the cause of the phenomenon because it is not a Gibbs energy; it is simply a signature of the role played by the hydrophobic effect. Therefore, the series of small 16-residue β-hairpins represents a good test case to confirm that the solvent-excluded volume is the actual ground of the hydrophobic effect and the main actor in determining the low temperature unfolding of both globular proteins and β-hairpins.

Theoretical description

To shed light on the conformational stability of a β-hairpin in aqueous solution, the following thermodynamic cycle has to be considered:

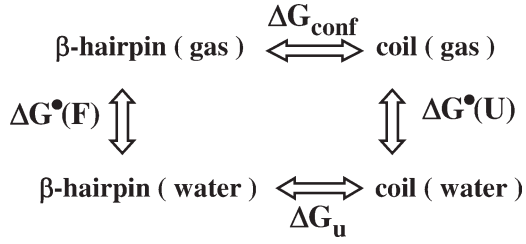

where F represents the folded conformation of the β-hairpin and U represents the ensemble of unfolded/coiled conformations of the peptide; ΔG_u is the Gibbs energy change associated with β-hairpin unfolding in water; ΔG_{conf} is the Gibbs energy change associated with β-hairpin unfolding in the gas phase:

$$\Delta G_{conf} = \Delta E_a(\text{intra}) - T\Delta S_{conf} \quad (1)$$

where $\Delta E_a(\text{intra}) = E_a(U|\text{intra}) - E_a(F|\text{intra})$ accounts for the difference in intra-peptide energetic interactions upon unfolding, and ΔS_{conf} represents the conformational entropy gain of the peptide chain upon unfolding; $\Delta G^\bullet(F)$ and $\Delta G^\bullet(U)$ are the Ben-Naim standard[16] Gibbs energy changes associated with the transfer from a fixed position in the gas phase to a fixed position in water (i.e., hydration) of the F-state and U-state, respectively. Application of equilibrium statistical thermodynamics leads to:[17,18]

$$\Delta G^\bullet(F) = \Delta G_c(F|\text{water}) + E_a(F|\text{water}) \quad (2)$$

$$\Delta G^\bullet(U) = \Delta G_c(U|\text{water}) + E_a(U|\text{water}) \quad (3)$$

where $\Delta G_c(F|\text{water})$ and $\Delta G_c(U|\text{water})$ represent the reversible work to create in water a cavity suitable to host the F-state and the U-state, respectively; $E_a(F|\text{water})$ and $E_a(U|\text{water})$ represent the energetic interactions (i.e., both van der Waals attractions, H-bonds and charge-dipole interactions) among the F-state or U-state and surrounding water molecules. Terms due to the reorganization of water-water H-bonds are not present in Eqs. (2) and (3) because this process does not affect the total Gibbs energy change, being characterized by a large enthalpy-entropy compensation.[19–21]

The thermodynamic cycle leads to the following expression for ΔG_u:

$$\begin{aligned}\Delta G_u &= \Delta G^\bullet(U) + \Delta G_{conf} - \Delta G^\bullet(F) \\ &= [\Delta G_c(U|\text{water}) - \Delta G_c(F|\text{water})] - T\cdot\Delta S_{conf} \\ &\quad + [E_a(U|\text{water}) - E_a(F|\text{water}) + \Delta E_a(\text{intra})] \quad (4)\end{aligned}$$

There is a balance for the energetic interactions between the U-state and the F-state, by taking into account both intrapeptide interactions and those with water molecules. Assuming that this balance is complete, the algebraic sum of the three energetic terms in the second square bracket of Eq. (4) is considered to be zero.[10] On this basis the ΔG_u expression becomes:

$$\begin{aligned}\Delta G_u &= [\Delta G_c(U|\text{water}) - \Delta G_c(F|\text{water})] - T\cdot\Delta S_{conf} \\ &= \Delta\Delta G_c - T\cdot\Delta S_{conf} \quad (5)\end{aligned}$$

The conformational stability of the β-hairpin over a large temperature range is determined by: (i) the reversible work to create in water a cavity suitable to host the peptide in its U-state and F-state, respectively; (ii) the conformational entropy gain of the chain upon unfolding. Since the U-state represents an ensemble of a large number of unfolded/coiled conformations, it is not simple to define a realistic model of the U-state and so a simple, analytic but reliable approach might be the right choice.

The creation of a cavity, at a fixed position in a liquid, keeping constant P, T, and the number of molecules, causes: (i) an increase in the average volume of the liquid by the cavity van der Waals volume, V_{vdW}; (ii) a marked decrease in the volume available to solvent molecules because the shell region between the cavity van der Waals surface and the solvent accessible surface of the cavity proves to be inaccessible to the center of solvent molecules in order to have V_{vdW} empty.[22] This inaccessible volume, V_{inacc}, leads to a solvent-excluded volume effect that is the real ground of the entropy cost of cavity creation. Geometric considerations indicate that: (i) V_{inacc} can be approximated by the solvent accessible surface area of the cavity,[22,23] $SASA_c$; (ii) a change in cavity shape, keeping fixed V_{vdW}, but increasing $SASA_c$, should cause a ΔG_c increase. This ΔG_c increase has been confirmed by means of both classic scaled particle theory,[24] SPT, calculations,[22] and molecular dynamics simulations using detailed water models.[25,26]

There is geometric commonality between β-hairpin folding and cavity shape change on keeping fixed V_{vdW}:[10]

the peptide chain undergoes a conformational transition but its van der Waals volume practically does not change, V_{vdW}(F-state) ≈ V_{vdW}(U-state). What changes on folding is V_{inacc} that can be measured by SASA, whose magnitude significantly decreases: SASA(F-state) ≪ SASA(*U*-state). It is important to underscore that the solvent-excluded volume effect has nothing to do with the chemical nature, polar or nonpolar of the surface groups, and the SASA change upon folding has not to be partitioned.[10]

Even though Eqs. (1)–(5) have been derived by explicitly considering water as solvent, it is important to perform the same calculations also in a common organic solvent, such as CCl_4 (the choice is simply dictated by the need to have a spherical solvent molecule as much as possible), to try to highlight what peculiar features of water play a role for β-hairpin conformational stability and occurrence of cold unfolding. All the above theoretical considerations can be translated in the following model and calculation procedure:

1. The unfolding process of β-hairpin is a conformational transition of the peptide chain whose V_{vdW} does not change on passing from the *F*-state to the *U*-state;

2. The *F*-state can be represented as a prolate spherocylinder with radius a = 4.0 Å and cylindrical length l = 20.0 Å (these values should be reliable on the basis of β-hairpin structure[12]), whereas the *U*-state can be represented as a prolate spherocylinder, having the same V_{vdW} of the one representing the *F*-state, but with radius a = 2.5 Å and cylindrical length l = 61.5 Å (this is a very crude representation of the ensemble of unfolded/coiled conformations,[27] but it should lead to clearer results and understanding);

3. The $\Delta\Delta G_c$ contribution can be estimated by calculating the reversible work to create in water and CCl_4 the corresponding cavities, using the classic SPT formula for spherocylinders[22] (the pressure-volume term is neglected for its smallness at P = 1 atm):

$$\begin{aligned}\Delta G_c = RT \cdot \{ &- \ln(1-\xi_1) + U(a/r_1) \\ &+ (U/4)\cdot(l/r_1) + U[1+(U/2)]\cdot(a/r_1)^2 \\ &+ (U/2)\cdot[1+(U/2)]\cdot[a\cdot l/(r_1)^2]\}\end{aligned} \quad (6)$$

where r_1 is the effective hard sphere radius of solvent molecules, the solvent volume packing density $\xi_1 = [4\pi(r_1)^3/3\cdot V_1]$, $U = 3\xi_1/(1-\xi_1)$, and V_1 is the solvent molar volume;

4. The $T\cdot\Delta S_{conf}$ contribution can be calculated in the assumption that each residue gains an average, temperature-independent and solvent-independent, conformational entropy upon unfolding:

$$T\cdot\Delta S_{conf} = T\cdot N_{res}\cdot\Delta S_{conf}(res) \quad (7)$$

where N_{res} = 16 for the selected β-hairpin, and $\Delta S_{conf(res)}$ = 27.3 J K^{-1}molres^{-1}; the latter number is approximately in the middle of the range defined for globular proteins by the average value, 14 J K^{-1}molres^{-1}, of the side chain entropy contribution,[28,29] and the average value, 40–50 J K^{-1}molres^{-1}, of the sum of backbone and side chain entropy contributions,[30,31] on the basis of different theoretical and experimental determination procedures.

RESULTS

The values of the effective hard sphere diameter of both water and CCl_4 molecules have been determined by fitting the experimental values of the isothermal compressibility β_T by means of the classic SPT formula for β_T.[32] The molar volume, isothermal compressibility, effective hard sphere diameter, and volume packing density for water and CCl_4, over the −30 to 100°C temperature range, are shown in Figure 1. Liquid water exists at 1 atm over this temperature range,[33] whereas for CCl_4 we have extrapolated experimental data covering the 0–75°C temperature range.[34] By looking at Figure 1, it is clear that σ_1 and ξ_1 present a parabolic-like temperature dependence in water with a maximum at 20°C, whereas they continuously decrease in CCl_4. These trends parallel those of the liquid density, shown in panel a of Figure 1 in terms of molar volume, with some modifications due to β_T. Specifically, in water, σ_1 = 2.61 Å and ξ_1 = 0.306 at −30°C, σ_1 = 2.715 Å and ξ_1 = 0.350 at 20°C, and σ_1 = 2.67 Å and ξ_1 = 0.318 at 100°C; in CCl_4, σ_1 = 5.26 Å and ξ_1 = 0.503 at −30°C, σ_1 = 5.15 Å and ξ_1 = 0.447 at 20°C, and σ_1 = 4.95 Å and ξ_1 = 0.355 at 100°C.

These σ_1 and ξ_1 numbers are used in Eq. (6) to calculate ΔG_c to create in water and CCl_4, over the −30 to 100°C temperature range and at 1 atm, cavities possessing the same V_{vdW}, but different shape in order to have different $SASA_c$. Specifically: (1) a spherocylindrical cavity of radius a = 4.0 Å and cylindrical length l = 20.0 Å; (2) a spherocylindrical cavity of radius a = 3.0 Å and cylindrical length l = 41.0 Å; (3) a spherocylindrical cavity of radius a = 2.5 Å and cylindrical length l = 61.5 Å. The relevant geometric features of these cavities are reported in Table I; note that: (i) the values of V_{excl}, V_{inacc}, and $SASA_c$ depend on the size of solvent molecules and increase on passing from water to CCl_4; (ii) by keeping fixed V_{vdW} and increasing the cylindrical length of the spherocylinder, the values of both V_{inacc} and $SASA_c$ increase markedly, regardless of the solvent. The obtained ΔG_c functions, shown in Figure 2, present: (a) a parabolic-like temperature dependence in water, with a flat maximum around 80°C, and a continuous linear decrease on increasing the temperature in CCl_4; (b) in both solvents the ΔG_c magnitude increases markedly with $SASA_c$, even though the cavity V_{vdW} is fixed, confirming the fundamental role played by the solvent-excluded volume effect;[22] (c) for the same spherocylindrical cavity, the ΔG_c values in water are larger than those in CCl_4, notwithstanding the

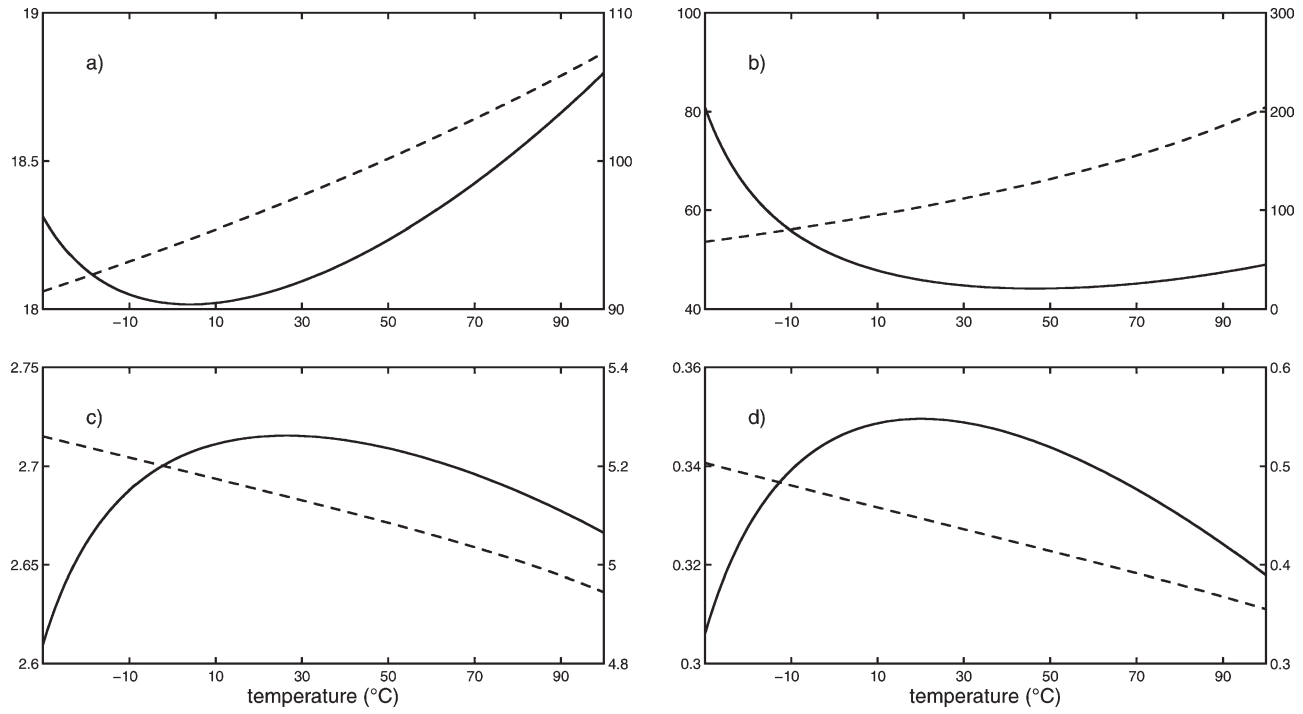

Figure 1

Temperature dependence of the molar volume in $cm^3\ mol^{-1}$ units (panel **a**), isothermal compressibility in $10^{12}{\cdot}cm^2\ dyne^{-1}$ units (panel **b**), effective hard sphere diameter in Å units (panel **c**), and volume packing density (panel **d**) for water (continuous lines to read on the left axis) and CCl_4 (dashed lines to read on the right axis).

larger $SASA_c$ in the latter solvent; this well-known result is basically due to the smaller size of water molecules with respect to those of CCl_4;[35,36] (d) a smaller size of solvent molecules implies that the number of solvent configurations that are incompatible with the solvent-excluded volume produced by the cavity is larger (a larger entropy penalty) in water than in CCl_4.

The ΔG_c decrease on lowering the temperature does not happen in CCl_4. The ΔG_c decrease in water is due to the combined effect of the temperature dependence of water density and isothermal compressibility β_T (note that the density decreases below TMD = 3.98°C, whereas β_T increases below about 40°C). These are peculiar fea-

Table I

Values of the Excluded Volume, Inaccessible Volume, and Solvent Accessible Surface Area in Water (First Line) and CCl_4 (Second Line) of Three Prolate Spherocylinders Possessing the Same van der Waals Volume

	Spherocylinder (1)	Spherocylinder (2)	Spherocylinder (3)
a (Å)	4	3	2.5
l (Å)	20	41	61.5
V_{vdW} (Å^3)	1273.4	1273.4	1273.4
V_{excl} (Å^3)	2491.8	2850.5	3187.2
	3941.3	4774.9	5580.9
V_{inacc} (Å^3)	1218.4	1577.1	1913.8
	2267.9	3501.5	4307.5
SASA (Å^2)	1045.0	1376.8	1698.2
	1376.8	1836.7	2297.6

The analytic formulas for a spherocylinder of radius a and cylindrical length l are: $V_{vdW} = (4/3)\pi a^3 + \pi l a^2$; $V_{excl} = [(4/3)\pi(a + r_1)^3] + [\pi l{\cdot}(a + r_1)^2]$; $V_{inacc} = V_{excl} - V_{vdW}$; $SASA = 4\pi(a + r_1)^2 + 2\pi l{\cdot}(a + r_1)$ where r_1 is the radius of solvent molecules, fixed at 1.4 Å for water, and 2.6 Å for CCl_4.

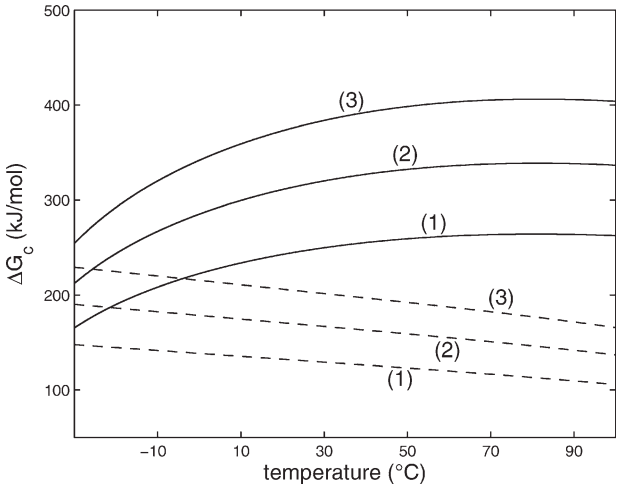

Figure 2

Temperature dependence of ΔG_c to create spherocylindrical cavities with (1) a = 4.0 Å and l = 20.0 Å; (2) a = 3.0 Å and l = 41.0 Å; (3) a = 2.5 Å and l = 61.5 Å in water (continuous lines) and CCl_4 (dashed lines).

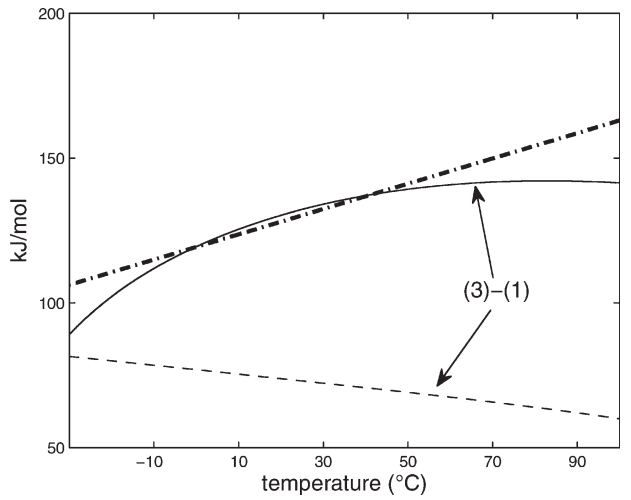

Figure 3

Temperature dependence of the functions $\Delta G_c(3) - \Delta G_c(1)$ in water (continuous line) and CCl_4 (dashed line). It is also shown the function $T{\cdot}\Delta S_{conf}$ calculated according to Eq. (7), by fixing $N_{res} = 16$ and $\Delta S_{conf(res)} = 27.3$ J K^{-1}molres^{-1} (dashed and dotted line); see text for further details.

tures of water, as emphasized by panels a and b of Figure 1, and are a consequence of the increase in tetrahedral order, that leads to a decrease in both σ_1 and ξ_1, rendering less costly the process of cavity creation.

Spherocylinder (1), with radius $a = 4.0$ Å and cylindrical length $l = 20.0$ Å, is assumed to correspond to the F-state of the β-hairpin; spherocylinder (3), with radius $a = 2.5$ Å and cylindrical length $l = 61.5$ Å, is assumed to be a model of the U-state of the peptide. Therefore, the $\Delta\Delta G_c$ term of Eq. (5) can be obtained by subtracting the ΔG_c values for spherocylinder (1) from those of spherocylinder (3). The obtained $\Delta\Delta G_c$ functions are reported in Figure 3 for both water and CCl_4: the two functions show the same temperature dependence already discussed for ΔG_c in each solvent. The continuous linear decrease of $\Delta\Delta G_c$ in CCl_4 does not allow the occurrence of cold unfolding because the $T{\cdot}\Delta S_{conf}$ term increases linearly with temperature according to Eq. (7). In contrast, the parabolic-like temperature dependence of $\Delta\Delta G_c$ in water is compatible with the occurrence of cold unfolding. In fact, the straight line of the $T{\cdot}\Delta S_{conf}$ term, calculated by fixing $N_{res} = 16$ and $\Delta S_{conf(res)} = 27.3$ J K^{-1}molres^{-1}, intersects the $\Delta\Delta G_c$ function in water at two temperatures, as emphasized in Figure 3. The difference between the two functions, reported in Figure 4, represents the thermodynamic stability curve of the β-hairpin, with $T_d(\text{cold}) \approx 0°C$, $T_d(\text{hot}) \approx 40°C$, $T_{max} \approx 20°C$ and $\Delta G_u(T_{max}) \approx 2.2$ kJ mol^{-1}. The temperature values are similar to those determined for small globular proteins,[37] whereas the $\Delta G_u(T_{max})$ number is markedly smaller than those obtained for small globular proteins, $\Delta G_d(T_{max}) = 25$–50 kJ mol^{-1}, confirming that an isolated β-hairpin has a low conformational stability.[12] By considering valid the reversible two-state model for the β-hairpin, $\Delta G_u(T_{max}) = 2.2$ kJ mol^{-1} implies that 70% of all the molecules populate the *F*-state at T_{max}. The latter value is not far from those obtained by means of a two-state analysis of circular dichroism and NMR data,[12–15] around 50%, for several variant forms of the 16-residue β-hairpin.

DISCUSSION

We have devised a simple model in which the *F*-state of an isolated β-hairpin is considered to be a spherocylinder with structurally reliable values for the radius and the cylindrical length, and the *U*-state of the 16-residue peptide is considered to be a thinner and longer spherocylinder but possessing the same V_{vdW} of that representing the *F*-state. Basic theoretical considerations allow us to single out two fundamental contributions for the conformational stability in aqueous solutions of the *F*-state: (i) the gain in configurational/translational entropy of water molecules due to the decrease in the solvent-excluded volume, measured by the SASA decrease upon folding; (ii) the loss in conformational entropy of the peptide chain in order to fix the φ, ψ, and χ dihedral angles upon folding. The first Gibbs energy term, $\Delta\Delta G_c$, has a parabolic-like temperature dependence in water and is crossed at two temperatures by the second Gibbs energy term, $T{\cdot}\Delta S_{conf}$, that increases linearly with temperature. Therefore: (i) the *F*-state is more stable than the *U*-state solely over the temperature range where the

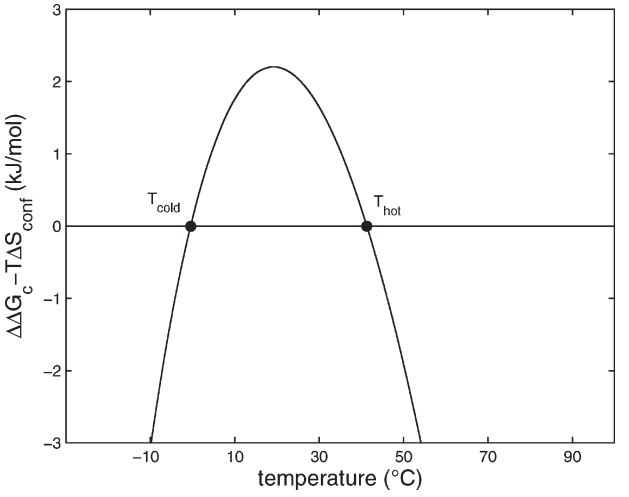

Figure 4

Thermodynamic stability curve of a model β-hairpin in water, obtained by subtracting the $T{\cdot}\Delta S_{conf}$ straight line from the $\Delta\Delta G_c = \Delta G_c(3) - \Delta G_c(1)$ curve, both reported in Figure 3. It shows the cold and hot unfolding temperatures.

$\Delta\Delta G_c$ term is larger than the $T{\cdot}\Delta S_{conf}$ term; (ii) cold unfolding is basically due to the significant decrease of $\Delta\Delta G_c$ on lowering the temperature, in particular below the TMD of water that, in turn, is mainly a consequence of the density decrease (i.e., the increase in molar volume shown in panel a of Fig. 1) for the increase in tetrahedral order. The parabolic-like temperature dependence of the ΔG_c and $\Delta\Delta G_c$ functions is a peculiar feature of water,[38–40] related to the strength of H-bonds and the openness of their 3D network. The ΔG_c and $\Delta\Delta G_c$ functions decrease in a linear and continuous manner in common organic solvents, such as CCl_4 [see Figs. 2(b) and 3] and n-hexane;[40] such a temperature dependence renders impossible the occurrence of cold unfolding, according to the devised model.

The assumption that the algebraic sum of the three energetic terms in the second square bracket of Eq. (4) is close to zero, merits more attention. In the isolated β-hairpin there are interstrand van der Waals contacts and H-bonds. Unfolding should destroy most of these intrapeptide interactions, but should allow the reformation of all of them with surrounding water molecules. On this basis it is safe to conclude that: (i) a balance between the three energetic terms in the second square bracket of Eq. (4) is operative in water and aqueous solutions; (ii) the assumption that this balance is complete could be acceptable since the analysis is qualitative in nature. If the three energetic terms do not cancel totally, the net remainder is likely to have only a small temperature dependence. This will have the effect of raising or lowering the $\Delta\Delta G_c$ curve in Figure 3 along the *y*-axis direction, leading to a shift in the values of unfolding temperatures, but it will not alter the conclusion that cold unfolding can happen by the proposed mechanism. Clearly, all such sentences are not true in organic solvents, such as CCl_4, whose molecules are not able to form H-bonds.

The overall entropy change upon unfolding is zero at the temperature where ΔG_u is maximum. The T_{max} value around 20°C obtained for the isolated β-hairpin in water is due to the balance of three entropy contributions: (i) the gain in conformational entropy of the peptide chain upon unfolding (that could be significantly affected by the introduction of point mutations); (ii) the loss in configurational/translational entropy of water molecules due to the increase in the solvent-excluded volume upon unfolding; (iii) a gain or a loss, depending on temperature, due to the reorganization of water–water H-bonds as a consequence of the change in cavity shape. Note that, in general, the temperature derivative of ΔG_c, in any liquid, consists of two terms:[41–43] one accounting for the decrease in the configurational/translational entropy of solvent molecules for the solvent-excluded volume produced by cavity creation; the other accounting for the structural reorganization of solvent molecules around the cavity. The latter term, according to classic SPT, is proportional to the thermal expansion coefficient, that in water is considered to be a measure of transient H-bond reorganization.[43] It is exactly the temperature dependence of this term to produce, according to SPT, the large and positive heat capacity change associated with the hydration of nonpolar species, and the unfolding of globular proteins and isolated β-hairpin.[1–5,12–15] It is worth noting that, notwithstanding the balance of the three energetic terms in the second square bracket of Eq. (4), according to the devised model, there is an enthalpy change associated with the two unfolding transitions, and amounts to about -64 kJ mol^{-1} at T_d(cold) $\approx$ 0°C, and to about 57 kJ mol^{-1} at T_d(hot) $\approx$ 40°C. It is due to the different extent of H-bond reorganization among the water molecules surrounding the *F*-state and the *U*-state (a difference caused by the different shape and so SASA of the two states). This enthalpy contribution, however, does not play an active role in the conformational transitions of the peptide chain because it is the manifestation of a process characterized by an almost complete enthalpy-entropy compensation.[19–21]

In conclusion, we have shown that the same theoretical approach devised to provide a molecular-level rationalization of cold denaturation in globular proteins[10] can account in a straightforward manner for the occurrence of cold unfolding in an isolated 16-residue β-hairpin in water. The decrease in the solvent-excluded volume upon folding, measured by SASA decrease, produces a large gain in configurational/translational entropy of water molecules that is the main stabilizing contribution of the folded conformation. This always stabilizing Gibbs energy contribution has a parabolic-like temperature dependence in water and is exactly counterbalanced at two temperatures (i.e., the cold and hot unfolding temperatures) by the always destabilizing Gibbs energy contribution due to the loss in conformational degrees of freedom of the peptide chain.

REFERENCES

1. Privalov PL, Griko YV, Venyaminov SY, Kutyshenko VP. Cold denaturation of myoglobin. J Mol Biol 1986;190:487–498.
2. Privalov PL. Cold denaturation of proteins. Crit Rev Biochem Mol Biol 1990;25:281–305.
3. Franks F. Protein destabilization at low temperatures. Adv Protein Chem 1995;46:105–109.
4. Pastore A, Martin SR, Politou A, Kondapalli KC, Stemmler T, Temussi PA. Unbiased cold denaturation: low- and high-temperature unfolding of yeast frataxin under physiological conditions. J Am Chem Soc 2007;129:5374–5375.
5. Sanfelice D, Tancredi T, Politou A, Pastore A, Temussi PA. Cold denaturation and aggregation: a comparative NMR study of titin I28 in bulk and in a confined environment. J Am Chem Soc 2009;131:11662–11663.
6. Graziano G, Catanzano F, Riccio A, Barone G. A reassessment of the molecular origin of cold denaturation. J Biochem 1997;122:395–401.
7. Riccio A, Ascolese E, Graziano G. Cold denaturation in the Schellman-Brandts model of globular proteins. Chem Phys Lett 2010; 486:65–69.

8. Chandler D. Interfaces and the driving force of hydrophobic assembly. Nature 2005;437:640–647.
9. Graziano G. Scaled particle theory study of the length scale dependence of cavity thermodynamics in different liquids. J Phys Chem B 2006;110:11421–11426.
10. Graziano G. On the molecular origin of cold denaturation of globular proteins. Phys Chem Chem Phys 2010;12:14245–14252.
11. Andersen NH, Cort JR, Liu Z, Sjoberg SJ, Tong H. Cold denaturation of monomeric peptide helices. J Am Chem Soc 1996;118: 10309–10310.
12. Maynard AJ, Sharman GJ, Searle MS. Origin of β-hairpin stability in solution: structural and thermodynamic analysis of the folding of a model peptide supports hydrophobic stabilization in water. J Am Chem Soc 1998;120:1996–2007.
13. Andersen NH, Dyer RB, Fesinmeyer RM, Gai F, Liu Z, Neidigh JW, Tong H. Effect of hexafluoroisopropanol on the thermodynamics of peptide secondary structure formation. J Am Chem Soc 1999;121:9879–9880.
14. Searle MS. Insights into stabilizing weak interactions in designed peptide β-hairpins. Biopolym Pept Sci 2004;76:185–195.
15. Dyer RB, Maness SJ, Franzen S, Fesinmeyer RM, Olsen KA, Andersen NH. Hairpin folding dynamics: the cold-denatured state is predisposed for rapid refolding. Biochemistry 2005;44:10406–10415.
16. Ben-Naim A. Solvation thermodynamics. New York: Plenum Press; 1987.
17. Lee B. Solvent reorganization contribution to the transfer thermodynamics of small nonpolar molecules. Biopolymers 1991;31:993–1008.
18. Graziano G. Benzene solubility in water: a reassessment. Chem Phys Lett 2006;429:114–118.
19. Ben-Naim A. Hydrophobic interaction and structural changes in the solvent. Biopolymers 1975;14:1337–1355.
20. Lee B. Enthalpy-entropy compensation in the thermodynamics of hydrophobicity. Biophys Chem 1994;51:271–278.
21. Lee B, Graziano G. A two-state model of hydrophobic hydration that produces compensating enthalpy and entropy changes. J Am Chem Soc 1996;118:5163–5168.
22. Graziano G. Dimerization thermodynamics of large hydrophobic plates: a scaled particle theory study. J Phys Chem B 2009;113:11232–11239.
23. Lee B, Richards FM. The interpretation of protein structures: estimation of static accessibility. J Mol Biol 1971;55:379–400.
24. Reiss H. Scaled particle methods in the statistical thermodynamics of fluids. Adv Chem Phys 1966;9:1–84.
25. Wallqvist A, Berne BJ. Molecular dynamics study of the dependence of water salvation free energy on solute curvature and surface area. J Phys Chem 1995;99:2885–2892.
26. Patel AJ, Varilly P, Chandler D. Fluctuations of water near extended hydrophobic and hydrophilic surfaces. J Phys Chem B 2010;114:1632–1637.
27. Gong H, Rose GD. Assessing the solvent-dependent surface area of unfolded proteins using an ensemble model. Proc Natl Acad Sci USA 2008;105:3321–3326.
28. Creamer TP, Rose GD. Side-chain entropy opposes alpha-helix formation but rationalizes experimentally determined helix-forming propensities. Proc Natl Acad Sci USA 1992;89:5937–5941.
29. Doig AJ, Sternberg MJE. Side-chain conformational entropy in protein folding. Protein Sci 1995;4:2247–2251.
30. Honig B, Yang AS. Free energy balance in protein folding. Adv Protein Chem 1995;46:27–58.
31. Privalov PL. Thermodynamic problems in structural molecular biology. Pure Appl Chem 2007;79:1445–1462.
32. Pierotti RA. On the scaled-particle theory of dilute aqueous solutions. J Phys Chem 1967;71:2366–2367.
33. Kell GS. Density, thermal expansivity, and compressibility of liquid water from 0 to 150°C: correlations and tables for atmospheric pressure and saturation reviewed and expressed on 1968 temperature scale. J Chem Eng Data 1975;20:97–105.
34. Cibulka I, Takagi T, Ruzicka K. P-ρ-T data of liquids: summarization and evaluation. VII. Selected halogenated hydrocarbons J Chem Eng Data 2001;46:2–28.
35. Lee B. The physical origin of the low solubility of nonpolar solutes in water. Biopolymers 1985;24:813–823.
36. Graziano G. Comment on reevaluation in interpretation of hydrophobicity by scaled particle theory. J Phys Chem B 2002;106:7713–7716.
37. Rees DC, Robertson AD. Some thermodynamic implications for the thermostability of proteins. Protein Sci 2001;10:1187–1194.
38. Garde S, Hummer G, Garcia AE, Paulaitis ME, Pratt LR. Origin of entropy convergence in hydrophobic hydration and protein folding. Phys Rev Lett 1996;77:4966–4968.
39. Graziano G, Lee B. Entropy convergence in hydrophobic hydration: a scaled particle theory analysis. Biophys Chem 2003;105:241–250.
40. Ashbaugh HS, Pratt LR. Contrasting nonaqueous against aqueous salvation on the basis of scaled-particle theory. J Phys Chem B 2007;111:9330–9336.
41. Lee B. A procedure for calculating thermodynamic functions of cavity formation from the pure solvent simulation data. J Chem Phys 1985;83:2421–2425.
42. Graziano G, Lee B. Hydration of aromatic hydrocarbons. J Phys Chem B 2001;105:10367–10372.
43. Graziano G. Entropy convergence in the hydration thermodynamics of *n*-alcohols. J Phys Chem B 2005;109:12160–12166.
44. Frank HS, Evans MW. Free volume and entropy in condensed systems. III. Entropy in binary liquid mixtures; partial molar entropy in dilute solutions; structure and thermodynamics of aqueous electrolytes. J Chem Phys 1945;13:507–532.
45. Kauzmann W. Some factors in the interpretation of protein denaturation. Adv Protein Chem 1959;14:1–63.
46. Graziano G, Lee B. On the intactness of hydrogen bonds around nonpolar solutes dissolved in water. J Phys Chem B 2005;109:8103–8107.
47. Finney JL, Bowron DT, Daniel RM, Timmins PA, Roberts MA. Molecular and mesoscale structures in hydrophobically driven aqueous solutions. Biophys Chem 2003;105:391–409.
48. Buchanan P, Aldiwan N, Soper AK, Creek JL, Koh CA. Decreased structure on dissolving methane in water. Chem Phys Lett 2005;415:89–93.
49. Filipponi A, Bowron DT, Lobban C, Finney JL. Structural determination of the hydrophobic hydration shell of Kr. Phys Rev Lett 1997;79:1293–1296.
50. Dec SF, Bowler KE, Stadterman LL, Koh CA, Sloan ED. Direct measure of the hydration number of methane. J Am Chem Soc 2006;128:414–415.
51. Qvist J, Halle B. Thermal signature of hydrophobic hydration dynamics. J Am Chem Soc 2008;130:10345–10353.
52. Graziano G. Case study of enthalpy-entropy non-compensation. J Chem Phys 2004;120:4467–4471.
53. Lum K, Chandler D, Weeks JD. Hydrophobicity at small and large length scales. J Phys Chem B 1999;103:4570–4577.
54. Rajamani S, Truskett TM, Garde S. Hydrophobic hydration from small to large lengthscale: understanding and manipulating the crossover. Proc Natl Acad Sci USA 2005;102:9475–9480.
55. Ashbaugh HS, Pratt LR. Scaled particle theory and length scales of hydrophobicity. Rev Mod Phys 2006;78:159–178.
56. Graziano G. Salting out of methane by sodium chloride: a scaled particle theory study. J Chem Phys 2008;129:084506.
57. Graziano G. Hydration entropy of polar, nonpolar and charged species. Chem Phys Lett 2009;479:56–59.
58. Graziano G. Role of salts on the strength of pairwise hydrophobic interaction. Chem Phys Lett 2009;483:67–71.

APPENDIX: SOME EXPLANATIONS ABOUT THE HYDROPHOBIC EFFECT

The low solubility of nonpolar solutes in water is the origin of the expression hydrophobic effect and, around room temperature, it is due to a large and negative entropy change accompanying the transfer of a solute from a fixed position in

the gas phase to a fixed position in water (i.e., the so called Ben-Naim standard[16,17]). This large and negative entropy change has to be rationalized at a molecular level. Frank and Evans[44] suggested, long time ago, that it is due to a structural reorganization of water molecules around the inserted nonpolar molecules, leading to an increased order of the H-bonded network (i.e., the pictorial iceberg model). This suggestion, with no experimental or computational/theoretical validation, was widely accepted and is still largely accepted by the biochemical community. Kauzmann[45] used it to indicate the hydrophobic effect as the fundamental driving force for the folding of globular proteins. Nonpolar side chains cluster together forming the core of native structure to reduce the entropic penalty experienced by water molecules when they are in contact with nonpolar moieties. However, there is no iceberg around nonpolar groups dissolved in water: first shell water molecules reorganize to avoid the waste of H-bonds, but this reorganization does not produce an order increase. [21,46] Direct structural investigations, such as neutron scattering, EXAFS and NMR measurements, [47–51] have unequivocally shown that the icebergs do not exist. Clearly, it remains the problem to identify the molecular origin of the large and negative entropy change pointed out above.

An entirely different theoretical explanation of hydrophobicity was originally developed by Lee on solid statistical mechanical grounds, [17,35] and subsequently strengthened by Graziano's applications and extensions. [18,22,36,39] The insertion of a nonpolar solute in water can be dissected in two sub-processes: (a) creation of a cavity suitable to host the solute molecule; (b) turning on solute-water van der Waals interactions. This dissection is dictated by physical considerations, [17,18] is not arbitrary, and is widely used. [8,38,40] The fundamental point is the recognition that the work of cavity creation, ΔG_c, is purely entropic in all liquids, [41] because it is a measure of the solvent-excluded volume produced by the cavity: the existence of the cavity reduces the configurational space available to liquid molecules, causing a significant loss in configurational/translational entropy. [9,22] In liquid phases a negative entropy change needs not be necessarily associated with a structure formation; it can be due to a decrease in available configurations. A structural reorganization of liquid molecules is always associated with cavity creation (note that it is distinct from the solvent-excluded volume effect), but it produces an enthalpy change that is exactly compensated for by a corresponding entropy change. [52] This has been demonstrated by means of a direct application of statistical mechanics,[9,41] and originates from the basic fact that cavities are produced by molecular-scale density fluctuations at equilibrium.

These are general features of the cavity creation process, but the latter has special features in water. First, ΔG_c in water is significantly larger than in common organic solvents: this is due to the small size of water molecules, [35,36] that enlarges the solvent-excluded volume effect (note that other authors[8,53–55] claim that this difference in ΔG_c magnitude is due to the larger liquid-vapour surface tension γ_∞ of water with respect to the other common liquids; but γ_∞ is a thermodynamic quantity not transparently linked to the solvation entropy, and so a molecular-level explanation has still to be provided by these authors). Second, ΔG_c has a parabolic-like temperature dependence in water, with a maximum around 80°C according to the calculation procedure used in this study, whereas it decreases almost linearly with temperature in common organic liquids.[40] This contrasting temperature dependence reflects the basic fact that: (a) on increasing the temperature, water density decreases to a markedly lesser extent with respect to that of common organic liquids; (b) water density shows a parabolic-like temperature dependence with a maximum at TMD = 3.98°C (these features are a consequence of the strength of H-bonds with respect to random thermal energy, and the openness of an ordered tetrahedral H-bonded network). The ΔG_c magnitude markedly depends on the liquid density and the size of liquid molecules, showing a parabolic-like temperature dependence in water with a maximum shifted to a significantly higher temperature with respect to TMD. In the last years, Chandler, Garde, Pratt and Ashbaugh[8,53–55] have shown that the hydrophobic effect is characterized by a marked lengthscale dependence: ΔG_c is proportional to cavity volume for small cavities, but to $SASA_c$ for large cavities (a cavity with $r_c = 10$ Å is considered to be large). This lengthscale dependence does not imply a change in mechanism as claimed by the above authors, it is a simple consequence of the fundamental role played by the solvent-excluded volume in all liquids, as already pointed out by Graziano.[9]

The theoretical approach devised by Lee and Graziano is able to quantitatively reproduce and rationalize the hydration thermodynamics of nonpolar solutes,[17,18,42] and other subtle features of hydrophobicity.[22,39,43,56–58] By recognizing that the folding of globular proteins is characterized by a large decrease in the solvent-excluded volume, the same theoretical approach can be extended to clarify the role of hydrophobic effect in determining the conformational stability of the native state.[10] This implies that the work of cavity creation and its temperature dependence play a pivotal role, and water is special with respect to common organic liquids for the same properties discussed above. Accordingly, the driving force of folding is the entropy gain of water molecules, as originally claimed by Kauzmann,[45] but the gain is the configurational/translational entropy from the decrease in solvent-excluded volume, not the orientational one from an imagined increase in the amount of H-bonded network.

It is worth noting that the parabolic-like temperature dependence of ΔG_c does not agree with the linear temperature decrease of γ_∞ of water.[40] This indicates that, by accepting that γ_∞ would be the main determinant of hydrophobicity,[8,53–55] it is not straightforward to explain the occurrence of cold denaturation. On the other hand, the iceberg idea has produced no numerical models that could really be tested against experimental data; it is therefore impossible to assess if this idea could explain the cold denaturation phenomenon.